THE JOURNAL OF NAVIGATION (2012), **65**, 59–72. © The Royal Institute of Navigation
doi:10.1017/S0373463311000531

On Modelling of Second-Order Ionospheric Delay for GPS Precise Point Positioning

Mohamed Elsobeiey and Ahmed El-Rabbany

(*Department of Civil Engineering, Ryerson University, 350 Victoria Street, Toronto, Canada M5B 2K3*)
(E-mail: rabbany@ryerson.ca)

Recent developments in GPS positioning show that a user with a standalone GPS receiver can obtain positioning accuracy comparable to that of carrier-phase-based differential positioning. Such technique is commonly known as Precise Point Positioning (PPP). A significant challenge of PPP, however, is that about 30 minutes or more is required to achieve centimetre to decimetre-level accuracy. This relatively long convergence time is a result of the un-modelled GPS residual errors. A major residual error component, which affects the convergence of PPP solution, is higher-order Ionospheric Delay (IONO). In this paper, we rigorously model the second-order IONO, which represents the bulk of higher-order IONO, for PPP applications. Firstly, raw GPS measurements from a global cluster of International GNSS Service (IGS) stations are corrected for the effect of second-order IONO. The corrected data sets are then used as input to the Bernese GPS software to estimate the precise orbit, satellite clock corrections, and Global Ionospheric Maps (GIMs). It is shown that the effect of second-order IONO on GPS satellite orbit ranges from 1·5 to 24·7 mm in radial, 2·7 to 18·6 mm in along-track, and 3·2 to 15·9 mm in cross-track directions, respectively. GPS satellite clock corrections, on the other hand, showed a difference of up to 0·067 ns. GIMs showed a difference up to 4·28 Total Electron Content Units (TECU) in the absolute sense and an improvement of about 11% in the Root Mean Square (RMS). The estimated precise orbit clock corrections have been used in all of our PPP trials. NRCan's GPSPace software was modified to accept the second-order ionospheric corrections. To examine the effect of the second-order IONO on the PPP solution, new data sets from several IGS stations were processed using the modified GPSPace software. It is shown that accounting for the second-order IONO improved the PPP solution convergence time by about 15% and improved the accuracy estimation by 3 mm.

KEY WORDS

1. GPS. 2. Precise Point Positioning. 3. Satellite Orbit. 4. Clock Corrections 5. Ionosphere.

1. INTRODUCTION. Traditionally, differential mode is used for GPS precise positioning applications. However, a major disadvantage of GPS differential positioning is its dependency on the measurements or corrections from a reference

receiver (i.e. two or more GPS receivers are required to be available). Unlike the differential mode where most GPS errors and biases are essentially cancelled, all errors and biases must be rigorously modeled in Precise Point Positioning (PPP). Typically, ionosphere-free linear combination of code and carrier-phase observations is used to remove the first-order ionospheric effect. This linear combination, however, leaves a residual Ionospheric Delay (IONO) component of up to a few centimeters representing higher-order ionospheric terms (Hoque and Jakowski, 2007, 2008). Satellite orbit and satellite clock errors can be accounted for using the International GNSS Service (IGS) precise orbit and clock products. Receiver clock error can be estimated as one of the unknown parameters. Effects of ocean loading, Earth tide, carrier-phase windup, sagnac, relativity, and satellite/receiver antenna phase-center variations can sufficiently be modeled or calibrated. Tropospheric delay can be accounted for by using empirical models (e.g. Saastamoinen or Hopfield models) or by using tropospheric corrections derived from regional GPS networks such as the National Oceanographic and Atmospheric Administration Tropospheric corrections (NOAATrop). The NOAATrop model incorporates GPS observations into Numerical Weather Prediction (NWP) models (Gutman et al., 2003).

At present, the IGS precise orbit and clock products do not take the second-order ionospheric delay into consideration. This leaves a residual error component, which is expected to slow down the convergence time and deteriorate the PPP solution. To overcome this problem, higher order IONO corrections must be considered when estimating the precise orbit and clock corrections, and when forming the PPP mathematical model. In this paper we restrict our discussion to the second-order IONO as it is much higher than all remaining higher order terms (Lutz et al., 2010). The second-order IONO results from the interaction of the ionosphere and the magnetic field of the Earth (Hoque and Jakowski, 2008). It depends on the Slant Total Electron Content (STEC), magnetic field parameters at the Ionospheric Pierce Point (IPP), and the angle between the magnetic field and the direction of signal propagation.

This paper estimates the second-order IONO and studies its impact on the accuracy of the estimated GPS satellite orbit, satellite clock corrections, and global ionospheric maps. In addition, the effect of accounting for the second-order IONO on the PPP solution is examined. It is shown that neglecting the second-order IONO introduces an error of up to 2 cm in the GPS satellite orbit and clock corrections and an error of up to 4·28 TECU in the estimated GIMs, based on DOY125 of recent (May 5, 2010) ionospheric and geomagnetic activities. In addition, accounting for the second-order IONO improves the PPP convergence time by about 15% and the accuracy of the estimated parameters by up to 3 mm.

2. GPS OBSERVATION EQUATIONS.

The mathematical models of undifferenced GPS pseudorange and carrier-phase measurements can found in Hofmann-Wellenhof et al. (2008) and Leick (2004). Considering the second-order IONO (Bassiri and Hajj, 2003) and satellite and receiver differential code bias (Schaer and Steigenberger, 2006; Dach et al., 2007), the mathematical models of undifferenced GPS pseudorange and carrier-phase measurements can be written as:

$$P_1 = \rho + c(dt_r - dt^s) + T + \frac{q}{f_1^2} + \frac{s}{f_1^3} + cd_{rP1} - 1{\cdot}546cDCB_{P1-P2} + dm_{P1} + e_1 \quad (1)$$

https://doi.org/10.1017/S0373463311000531 Published online by Cambridge University Press

$$P_2 = \rho + c(dt_r - dt^s) + T + \frac{q}{f_2^2} + \frac{s}{f_2^3} + cd_{rP2} - 2{\cdot}546cDCB_{P1-P2} + dm_{P2} + e_2 \quad (2)$$

$$\begin{aligned}\Phi_1 =& \rho + c(dt_r - dt^s) + T - \frac{q}{f_1^2} - \frac{s}{2f_1^3} + \lambda_1 N_1 \\ &+ c(\delta_{r1} + \delta_1^s - 2{\cdot}546d_{P1}^s + 1{\cdot}546d_{P2}^s) + \delta m_1 + \varepsilon_1\end{aligned} \quad (3)$$

$$\begin{aligned}\Phi_2 =& \rho + c(dt_r - dt^s) + T - \frac{q}{f_2^2} - \frac{s}{2f_2^3} + \lambda_2 N_2 \\ &+ c(\delta_{r2} + \delta_2^s - 2{\cdot}546d_{P1}^s + 1{\cdot}546d_{P2}^s) + \delta m_2 + \varepsilon_2\end{aligned} \quad (4)$$

where, P_1, P_2 are pseudorange measurements on L1 and L2, respectively; Φ_1,Φ_2 are carrier-phase measurements on L1 and L2, respectively, scaled to distance (m); f_1, f_2 are L1 and L2 frequencies, respectively, (L_1:$f_1 = 1{\cdot}57542\ GHz$; L_2:$f_2 = 1{\cdot}22760\ GHz$); dt_r, dt^s are receiver and satellite clock errors, respectively; dm_1, dm_2 are code multipath effect; δm_1, δm_2 are carrier-phase multipath effect; e_1, e_2, ε_1, ε_2 are the un-modeled error sources; λ_1, λ_2 are the wavelengths for L1 and L2 carrier frequencies, respectively; N_1, N_2 are integer ambiguity parameters for L1 and L2, respectively; DCB is the satellite Differential Code Bias; δ_r, $\delta^s$are frequency-dependent carrier-phase hardware delay for receiver and satellite, respectively; d_r, $d^s$are code hardware delay for receiver and satellite, respectively; c is the speed of light in vacuum; and ρ is the true geometric range from receiver antenna phase-centre at reception time to satellite antenna phase-centre at transmission time (m); q expresses the Total Electron Content (TEC) integrated along the line of sight (i.e. $q = 40.3\int N_e\, dl = 40.3 * STEC$); N_e is the electron density (electrons/m^3); s represents the second-order ionospheric effect; $STEC$ is the Slant Total Electron Content.

The well-known ionosphere-free linear combination can be formed to eliminate the first-order IONO as,

$$P_{IF} = \rho^{\backslash} + T + \frac{s}{f_1 f_2 (f_1 + f_2)} + e_{IF} \quad (5)$$

$$\Phi_{IF} = \rho^{\backslash} + T - \frac{s}{2f_1 f_2 (f_1 + f_2)} + \varepsilon_{IF} \quad (6)$$

$$s = 7527 * c * B_0 * \cos(\theta) * STEC \quad (7)$$

where, P_{IF}, Φ_{IF} are the first-order ionosphere-free code and carrier-phase combinations, respectively; $\rho^{\backslash}$ includes the geometric range, receiver and satellite clock errors; e_{IF}, ε_{IF} are the first-order ionosphere-free combination of e_1, e_2 and ε_1, ε_2, respectively; B_0 is the magnetic field at the IPP (i.e. the intersection of the line of sight with the ionospheric single layer at height h_{ion}) and θ is the angle between the magnetic field and the propagation direction (Figure 1).

3. COMPUTATION OF STEC. Equations 5 through 7 show that the second-order IONO depends on the STEC along the line of sight and the magnetic field parameters at the IPP. STEC values may be obtained from agencies such as the IGS and NOAA. IGS produces Global Ionospheric Maps (GIMs) in the Ionospheric Exchange (IONEX) format (Schaer et al., 1998). GIMs are produced

https://doi.org/10.1017/S0373463311000531 Published online by Cambridge University Press

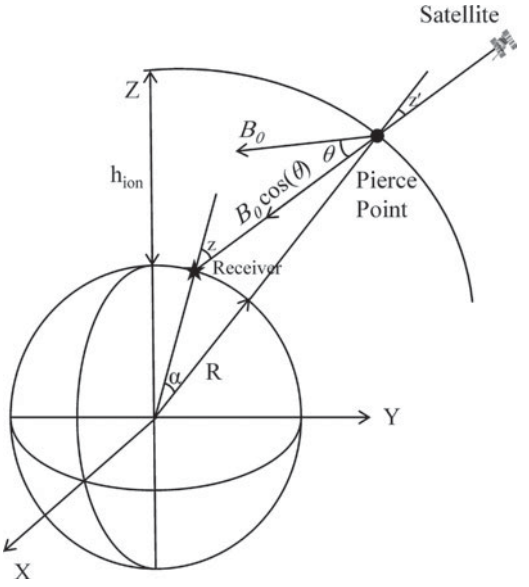

Figure 1. Magnetic Field and Propagation Direction.

with a 2-hour temporal resolution and a 2·5° (latitude) by 5° (longitude) spatial resolution on a daily basis as rapid global maps. The rapid global maps are available with a delay less than 24 hours and accuracy in the order of 2–9 TECU, while the final maps are available with a delay about 11 days and accuracy in the order of 2–8 TECU (http://igscb.jpl.nasa.gov/components/prods.html). GIMs provide the Vertical Total Electron Content (VTEC) that has to be converted to STEC using a mapping function. STEC computed using the GIM model can introduce up to 50% error at low latitude and low elevations (Hernández-Pajares et al., 2007). NOAA, on the other hand, produces a regional ionospheric model known as the United States Total Electron Content (US-TEC). US-TEC covers regions across the Continental US (CONUS), extending from latitude 10° to 60° North and from longitude 50° to 150° West. The US-TEC maps have a spatial resolution of 1° × 1° and a temporal resolution of 15 minutes (Rowell, 2005). The maps include both STEC and VTEC for different locations and directions. The accuracy of the US-TEC maps is in the range of 1 to 3 TECU. The differential VTEC has an average Root Mean Square Error (RMSE) of 1·7 TECU, which is equivalent to less than 30 cm of signal delay at the GPS L1 frequency. Differential STEC, on the other hand, has an average RMSE of 2·4 TECU, which is equivalent to less than 40 cm of signal delay at the GPS L1 frequency.

Alternatively, STEC can be estimated by forming the geometry-free linear combination of GPS pseudorange observables (Equation 8). However, this method requires *a priori* information about satellite and receiver differential code biases ($DCB^S{}_{P1-P2}$, DCB_{rP1-P2}, respectively). Values of satellite and receiver differential code biases ($DCB^S{}_{P1-P2}$, DCB_{rP1-P2}, respectively) may be obtained from the IGS or estimated by processing the GPS data from a well-distributed global network of GPS stations. Satellite and receiver differential code biases are stable over time and

https://doi.org/10.1017/S0373463311000531 Published online by Cambridge University Press

previous values may be used (Hernández-Pajares et al., 2007).

$$STEC = \left[(P_2 - P_1) + c(DCB_{rP1-P2} + DCB^{S}_{P1-P2})\right]\left(\frac{f_2^2}{f_1^2 - f_2^2}\right)\left(\frac{f_1^2}{40.3}\right) \quad (8)$$

Where, DCB_{rP1-P2} represents the receiver differential hardware delay between P1 and P2 pseudoranges; DCB^{S}_{P1-P2} represents the satellite differential hardware delay between P1 and P2 pseudoranges.

4. MAGNETIC FIELD MODEL. The geomagnetic field of the Earth can be approximated by a magnetic dipole placed at the Earth's centre and tilted 11·5° with respect to the axis of rotation. The magnetic field inclination is downwards throughout most of the northern hemisphere and upwards throughout most of the southern hemisphere. A line that passes through the centre of the Earth along the dipole axis intersects the surface of the Earth at two points, referred to as the geomagnetic poles. Unfortunately, the dipole model accounts for about 90% of the Earth's magnetic field at the surface (Merrill and McElhinny, 1983). After the best fitting geocentric dipole is removed from the magnetic field at the Earth's surface, the remaining part of the field, about 10%, is referred to as non-dipole field. Both dipole and non-dipole parts of the Earth's magnetic field change with time (Merrill and McElhinny, 1983). The dipole approximation is more or less valid up to a few Earth radii; beyond this distance limit the Earth's magnetic field significantly deviates from the dipole field because of the interaction with the magnetized solar wind (Houghton et al., 1998).

A more realistic model for the Earth's geomagnetic field, which is used in this paper, is the International Geomagnetic Reference Field (IGRF). The IGRF model is a standard spherical harmonic representation of the Earth's main field. The model is updated every 5 years. The International Association of Geomagnetism and Astronomy (IAGA) released the 11th generation of the IGRF in December 2009. The coefficients of the IGRF11 model are based on data collected from different sources, including geomagnetic measurements from observatories, ships, aircraft, and satellites (NOAA, 2010). The relative difference between the dipole and IGRF models ranges from −20% in the east of Asia up to +60% in the so-called south Atlantic anomaly (Hernández-Pajares et al., 2007).

5. EFFECT OF SECOND-ORDER IONOSPHERIC DELAY ON THE DETERMINATION OF SATELLITE ORBIT AND CLOCK CORRECTIONS. To investigate the effect of second-order IONO on the GPS satellite orbit and clock corrections, Bernese GPS software was used. A global cluster of 284 IGS reference stations (Figure 2) was formed based on *a priori* information about the behaviour of each receiver's clock and the total number of carrier-phase ambiguities in the corresponding observation files. GPS measurements collected at the 284 IGS stations were downloaded from the IGS website for May 05, 2010 (DOY125). The raw data were first corrected for the effect of second-order IONO using Equations 5 through 7. Equation 8 was used to compute the STEC values and the IGS published Differential Code Biases (DCBs) were applied. The corrected data along with the broadcast ephemeris were used as input to the Bernese GPS software to estimate the satellite orbit and clock corrections. Our results showed that the effect of second-order

https://doi.org/10.1017/S0373463311000531 Published online by Cambridge University Press

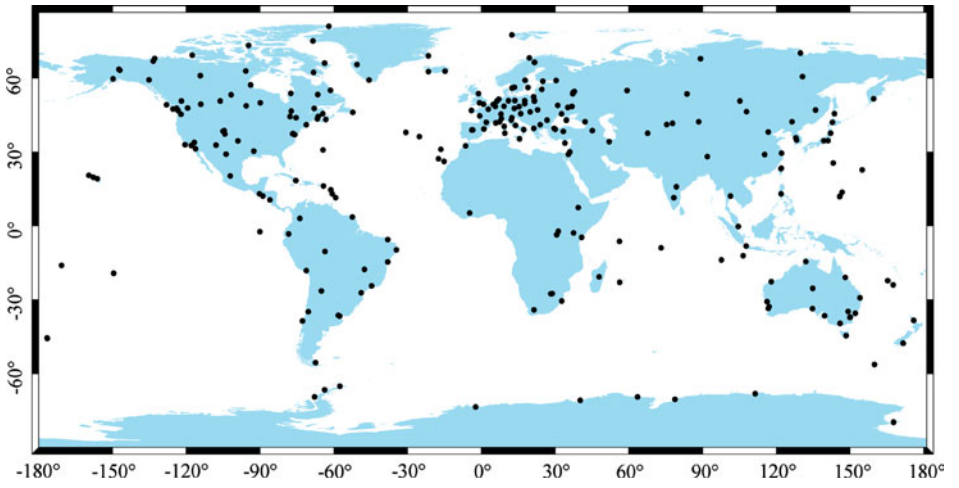

Figure 2. Global Cluster of IGS Stations Used in Estimation of GPS Satellite Orbit, Satellite Clock Corrections, and GIMs.

IONO on GPS satellite orbit ranges from 1·5 to 24·7 mm in radial, 2·7 to 18·6 mm in the along-track, and 3·2 to 15·9 mm in cross-track directions, respectively (Table 1).

Because only the difference between receiver and satellite clock parameters $c(dt_r - dt^s)$ appears in the GPS observation equations, it is only possible to solve for the clock parameters in the relative sense. All clock parameters but one can be estimated (i.e. either a receiver or a satellite clock correction has to be fixed or selected as a reference). The only requirement is that the reference clock must be available for each epoch where the clock values are estimated (Dach et al., 2007). A reference clock should be easily modelled by an offset and a drift. A polynomial is fitted to the combined values of the clock corrections. In this way the time scale presented by the reference clock is the same for the entire solution. When the reference clock is synchronized to the GPS broadcast time, all aligned clocks to the reference clock will refer to the same time scale. All deviations of the real behaviour of the reference clock are reflected in all other clocks of the solution; therefore, the reference clock must be carefully selected. To determine the reference clock, Bernese GPS software fits a polynomial of the first-order as a default (with the option to use up to the 10^{th} order) to all clocks and the mean Root Mean Square (RMS) is computed. The reference clock is selected as the clock which leads to the smallest mean fit RMS and is available for all epochs.

Our study showed that the effect of second-order IONO on the estimated satellite clock solution differences were within 0·067 ns (2 cm). Table 2 shows the RMS (in picoseconds) of the estimated satellites clock corrections (Est.) compared with the corresponding values of the IGS final satellites clock corrections.

6. EFFECT OF SECOND-ORDER IONOSPHERIC DELAY ON GIM ESTIMATES.

Typically, the IONO can be broken down into two components: deterministic and stochastic. The deterministic component of the IONO is usually based on the Single-Layer Model (SLM) as shown in Figure 1.

https://doi.org/10.1017/S0373463311000531 Published online by Cambridge University Press

Table 1. Effect of Second-Order Ionospheric Delay on GPS Satellite Orbit.

	Orbit Difference (mm)				Orbit Difference (mm)		
PRN	Radial	Along-Track	Cross-Track	PRN	Radial	Along-Track	Cross-Track
G02	11·1	8·1	3·2	G17	1·5	8	3·4
G03	19·8	2·7	5·8	G18	5·1	3	6·5
G04	19·7	4·7	6·4	G19	21	5·5	9
G05	24·7	3·5	8·3	G20	3·6	12·3	15·9
G06	9	4·8	5·6	G21	2·7	7	3·4
G07	14	4·8	6·7	G22	3·2	5·4	9·8
G08	20	18·6	9	G23	8·6	11·5	4·5
G09	11·6	4·9	7·9	G24	2·6	7·3	4·8
G10	13·1	5	8·2	G26	5·3	2·8	6·1
G11	7	10·6	9·7	G27	9·6	3	8·4
G12	22·1	8·9	4·8	G28	14·9	10	6·3
G13	6·8	5·3	8·4	G29	6·7	4·9	3·3
G14	4·5	7·9	4·5	G30	4·1	4·8	6·7
G15	16·3	4·4	5·3	G31	4·9	3·3	12·9
G16	2·4	4·7	3·6	G32	3·2	10·9	8·3

Table 2. RMS of GPS Satellites Clock Corrections.

	Clock RMS (ps)			Clock RMS (ps)	
PRN	IGS	Est.	PRN	IGS	Est.
G02	20·74	3·82	G17	15·88	3·85
G03	16·53	3·87	G18	12·03	4·64
G04	19·05	3·95	G19	26·42	3·91
G05	15·23	3·87	G20	12·64	3·82
G06	15·25	4·73	G21	25·17	3·66
G07	17·74	3·74	G22	12·83	4·39
G08	18·19	4·21	G23	28·45	3·70
G09	41·10	4·11	G24	18·99	3·68
G10	13·94	3·86	G26	18·31	4·00
G11	15·53	4·08	G27	13·51	4·03
G12	23·32	3·73	G28	14·65	4·21
G13	16·95	3·69	G29	13·15	4·21
G14	13·37	4·95	G30	19·24	3·84
G15	16·42	3·97	G31	18·18	4·91
G16	16·18	3·97	G32	27·83	3·77

This model assumes that all free electrons are concentrated in a shell of infinitesimal thickness. The stochastic component, on the other hand, can be interpreted as the short-term TEC variations. It can be expressed as the IONO term of the double-difference observation equations (Dach et al., 2007). The global TEC model can be written as:

$$E(\beta, s) = \sum_{n=0}^{n_{\max}} \sum_{m=0}^{n} \tilde{P}_{nm}(\sin\beta)(a_{nm}\cos ms + b_{nm}\sin ms)$$

https://doi.org/10.1017/S0373463311000531 Published online by Cambridge University Press

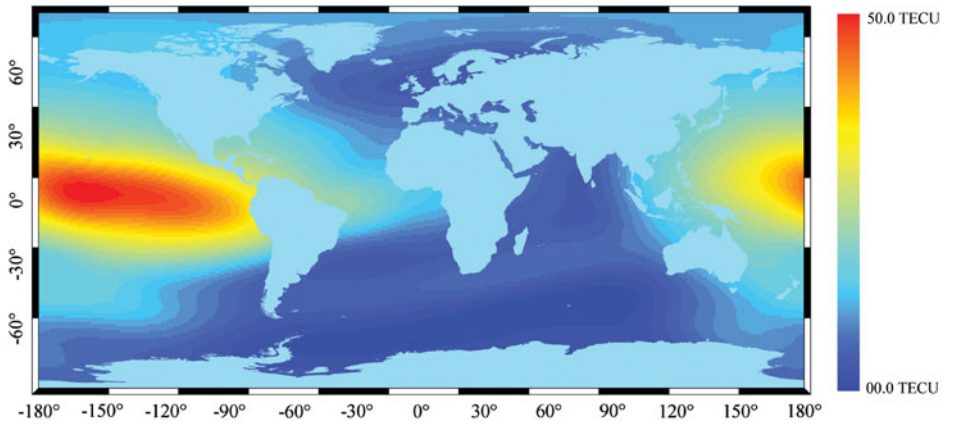

Figure 3. Estimated GIM at 00 h (GMT Time) DOY125, 2010.

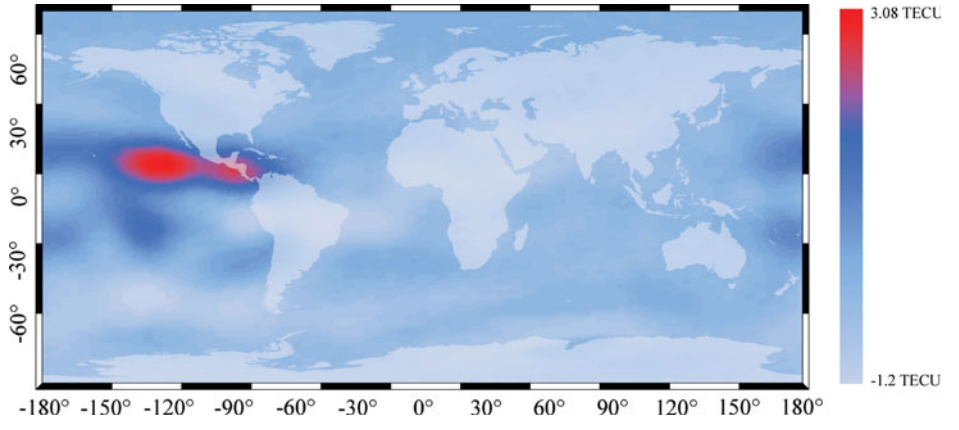

Figure 4. Effect of Second-Order Ionospheric Delay (IONO) on GIM at 00 h (GMT Time) DOY125, 2010.

where, β is the geographic latitude, s is the sun-fixed longitude, $n_{\max}$ is the maximum degree of the spherical harmonic expansion, $\tilde{P}_{nm} = \Lambda(n, m)P_{nm}$ are the normalized associated Legendre functions of degree n and order m, based on normalization function $\Lambda(n, m)$ and Legendre functions P_{nm}, a_{nm}, b_{nm} are the unknown TEC coefficients of the spherical harmonics (i.e. the global ionospheric model parameters to be estimated).

GIM is estimated from the previously described global cluster (Figure 2) using the Bernese GPS software. Our results indicate that neglecting second-order IONO can cause an error of up to 4·28 TECU, in the absolute sense, in the estimated GIM values. Also, accounting for the second-order IONO improves the RMS of the estimated GIMs by 11%. Figure 3 shows the estimated GIM at time 00 h (GMT) on May 5, 2010. Figure 4, on the other hand, shows the effect of second-order IONO on GIM estimation at the same time. It can be seen that most of the effect is concentrated

https://doi.org/10.1017/S0373463311000531 Published online by Cambridge University Press

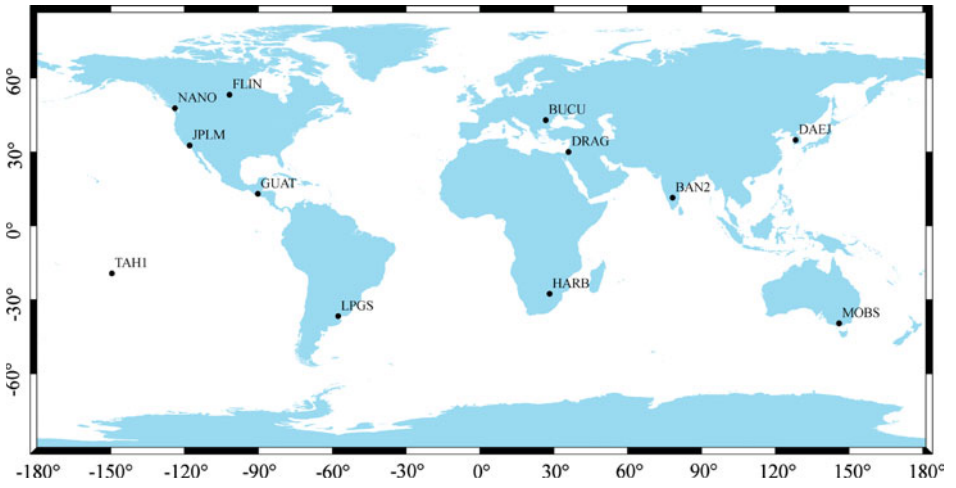

Figure 5. IGS Stations Used in Examining the Effect of Second-Order Ionospheric Delay (IONO) on PPP Solution.

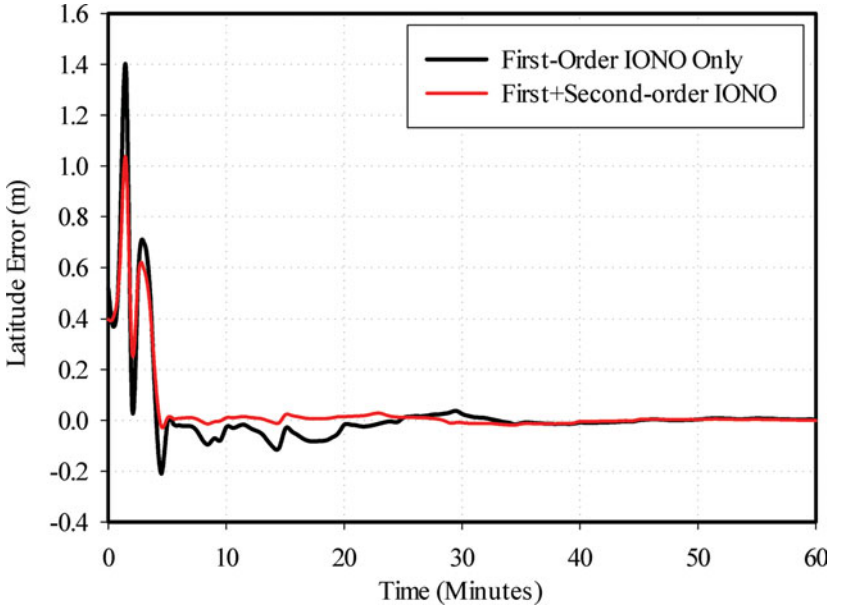

Figure 6. Latitude Improvement Due to Accounting for Second-Order Ionospheric Delay (IONO) at DRAG Station, DOY125, 2010.

according to the Sun-Earth relative position. This behaviour is expected as the second-order IONO is dependent on the TEC and magnetic field conditions.

7. EFFECT OF SECOND-ORDER IONOSPHERIC DELAY ON PPP SOLUTION.

The GPSPace PPP processing software, which was developed

https://doi.org/10.1017/S0373463311000531 Published online by Cambridge University Press

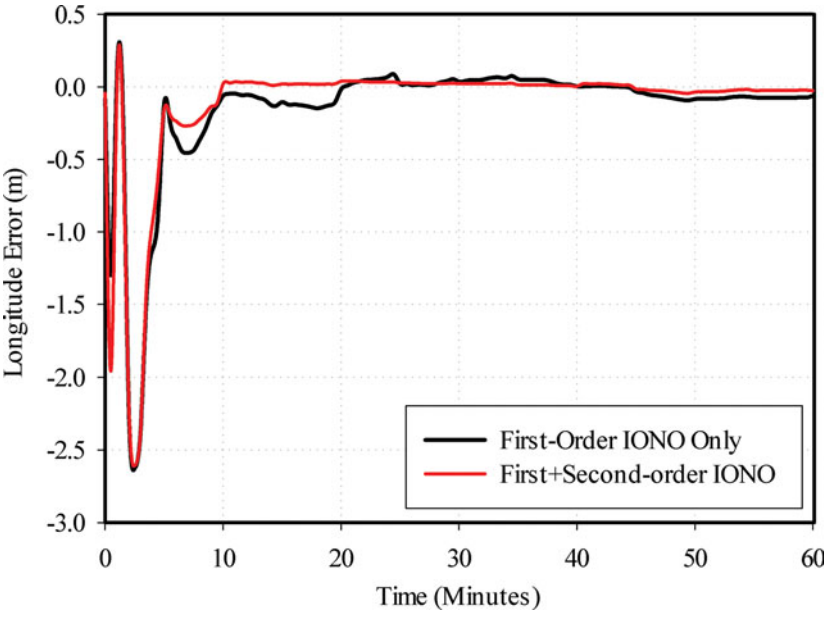

Figure 7. Longitude Improvement Due to Accounting for Second-Order Ionospheric Delay (IONO) at DRAG Station, DOY125, 2010.

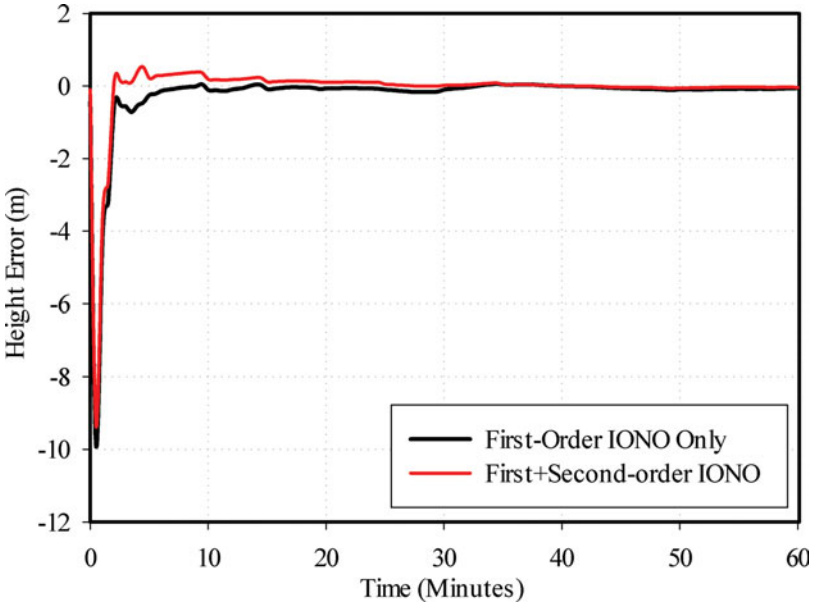

Figure 8. Ellipsoidal Height Improvement Due to Accounting for Second-Order Ionospheric Delay (IONO) at DRAG Station, DOY125, 2010.

by Natural Resources Canada (NRCan), was modified to accept the second-order ionospheric correction. To examine the effect of second-order IONO on the PPP solution, GPS data from 12 IGS stations (Figure 5) were processed using the modified

https://doi.org/10.1017/S0373463311000531 Published online by Cambridge University Press

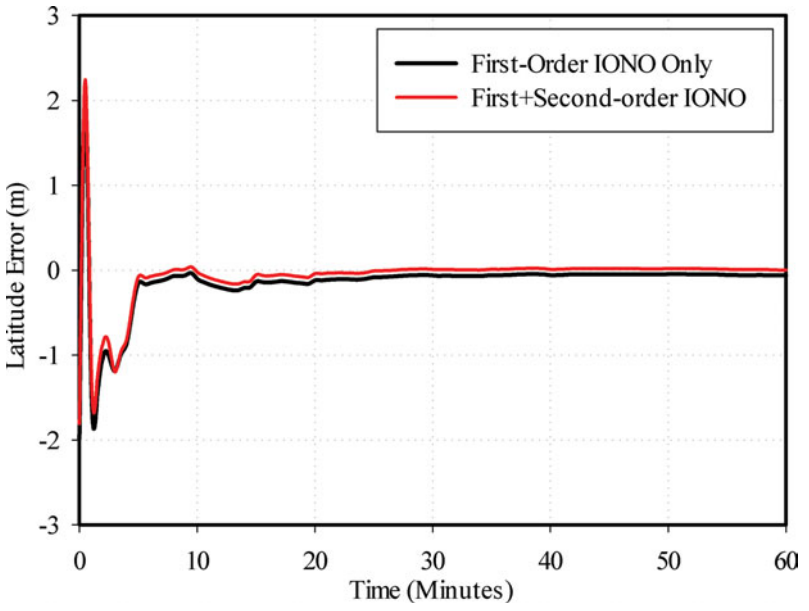

Figure 9. Latitude Improvement Due to Accounting for Second-Order Ionospheric Delay (IONO) at THA1 Station, DOY125, 2010.

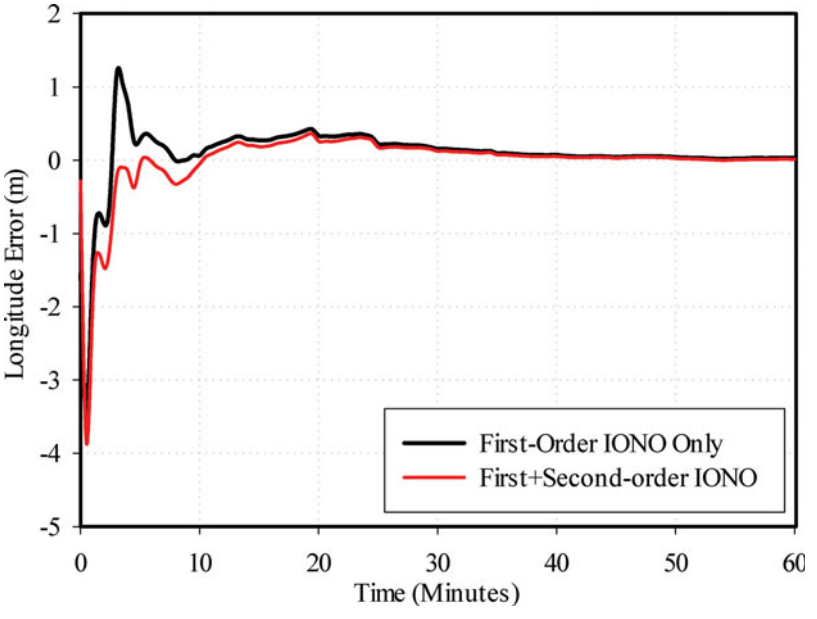

Figure 10. Longitude Improvement Due to Accounting for Second-Order Ionospheric Delay (IONO) at THA1 Station, DOY125, 2010.)

https://doi.org/10.1017/S0373463311000531 Published online by Cambridge University Press

Table 3. RMS of Final PPP Solution for Tested IGS Stations.

Processing Mode	1st Order IONO RMS (mm)				1st and 2nd Order IONO RMS (mm)			
Station	Lat.	Lon.	Ht.	3D	Lat.	Lon.	Ht.	3D
BAN2	2·1	2·5	3·1	4·5	1	1·2	1·8	2·4
BUCU	1·2	2	2·6	3·5	0·8	1·9	2	2·9
DAEJ	2	2·2	2·9	4·2	0·5	0·8	1·3	1·6
DRAG	2·2	2·4	3·3	4·6	1·1	0·9	1·2	1·9
FLIN	2	2·1	2·3	3·7	1·8	1·9	2	3·3
GUAT	2	2·8	3·5	4·9	0·6	1·9	2·1	2·9
HARB	1·5	1·5	1·8	2·8	1·2	1·4	1·5	2·4
JPLM	1·1	1·8	1·9	2·8	1	1·5	1·6	2·4
LPGS	1·7	2·1	2·8	3·9	1·1	1·8	2	2·9
MOBS	1·5	1·7	2·2	3·2	1·2	1·4	1·8	2·6
NANO	1·8	2·2	2·7	3·9	1·2	2	2·5	3·4
TAH1	1·2	2·1	2·4	3·4	0·9	1·8	2	2·8

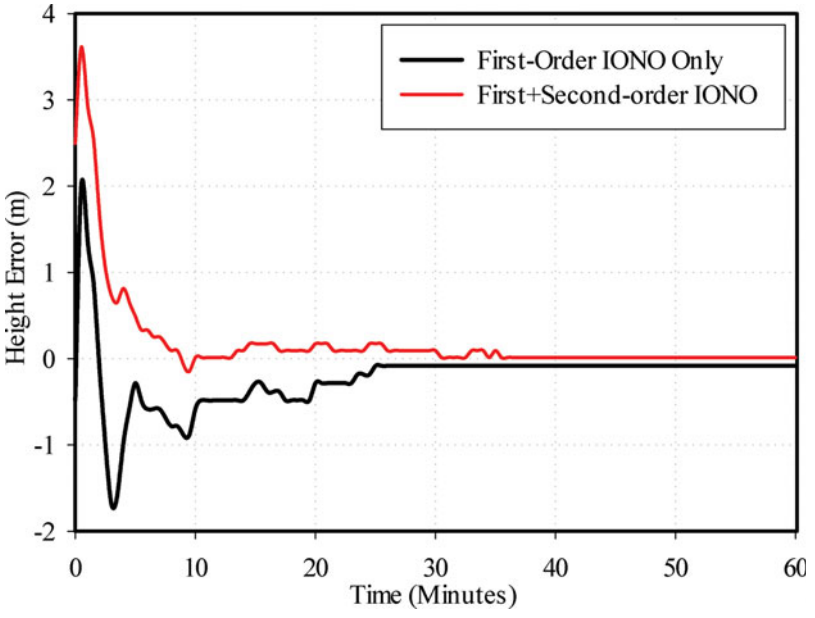

Figure 11. Ellipsoidal Height Improvement Due to Accounting for Second-Order Ionospheric Delay (IONO) at THA1 Station, DOY125, 2010.

GPSPace. The stations were chosen randomly and were not included in the estimation of satellite orbit and clock corrections. The data used were the ionosphere-free (with both first- and second-order corrections included) linear combination of pseudorange and carrier-phase measurements. The estimated precise satellite orbit and clock corrections, from the previous step, were used in the data processing. The results show that improvements are attained in all three components of the station coordinates. Figures 6 to 11 show the 3D solutions obtained with and without the second-order ionospheric corrections included, for stations THA1 and DRAG as examples. As

https://doi.org/10.1017/S0373463311000531 Published online by Cambridge University Press

can be seen, the amplitude variation of the estimated coordinates during the first 15 minutes is reduced when considering the second-order IONO. In addition, the convergence time for the estimated parameters is reduced by about 15%. The final PPP solution shows an improvement in the order of 3 mm in station coordinates. It should be pointed out that the solution improvement is much higher at low latitudes where the second-order ionospheric effect is much higher (see Figure 4). Table 3 summarizes the RMS of the final solution of all stations.

8. CONCLUSIONS. It has been shown that rigorous modelling of GPS residuals error can improve the PPP convergence time and solution. It has been shown that neglecting the second-order Ionospheric Delay (IONO) can produce an orbital error ranging from 1·5 to 24·7 mm in radial, 2·7 to 18·6 mm along-track, and 3·2 to 15·9 mm in cross-track directions, respectively. Also, neglecting the second-order IONO results in a satellite clock error of up to 0·067 ns (i.e. equivalent to a ranging error of 2 cm). Moreover, neglecting the second-order IONO can cause an absolute error of up to 4·28 TECU (i.e. equivalent to ranging error of 0·70 m on L1 frequency observations) in GIM values. Furthermore, accounting for the second-order IONO can improve the final PPP coordinate solution by about 3 mm and improve the convergence time of the estimated parameters by about 15% .

ACKNOWLEDGEMENTS

This research was supported in part by the GEOIDE Network of Centres of Excellence (Canada) and by the Natural Sciences and Engineering Research Council (NSERC) of Canada. The authors would like to thank the Geodetic Survey Division of NRCan for providing the source code of the GPSPace PPP. The data sets used in this research were obtained from the IGS website http://igscb.jpl.nasa.gov/.

REFERENCES

Bassiri, S. and Hajj, G. (1993). High-order ionospheric effects on the global positioning system observables and means of modeling them, *Manuscr. Geod.*, **18**, 280–289.

Dach, R., Hugentobler, U., Fridez, P. and Meindl, M. (2007). Bernese GPS Software Version 5.0. Astronomical Institute, *University of Berne, Switzerland*.

Gutman, S., Fuller-Rowell, T. and Robinson, D. (2003). Using NOAA Atmospheric Models to Improve Ionospheric and Tropospheric Corrections. *U.S. Coast Guard DGPS Symposium, Portsmouth, VA*.

Hernández-Pajares, M., Juan, J. M., Sanz, J. and Orús, R. (2007). Second-order Ionospheric Term in GPS: Implementation and Impact on Geodetic Estimates. *Journal of Geophysical Research*, **112**, B08417.

Hofmann-Wellenhof, B., Lichtenegger, H. and Walse, E. (2008). *GNSS Global Navigation Satellite Systems; GPS, Glonass, Galileo & More*. Springer Wien, New York.

Hoque, M. and Jakowski, N. (2007). Higher order ionospheric effects in precise GNSS positioning. *Journal of Geodesy*, **81**, 259–268.

Hoque, M. and Jakowski, N. (2008). Mitigation of higher order ionospheric effects on GNSS users in Europe. *GPS Solutions*, **12**–**2**, 87–97.

Houghton, J. T., Rycroft, M. J. and Dessler, A. J. (1998). *Physics of the Space Environment*. Cambridge University Press, 1998.

Leick, A. (2004). *GPS Satellite Surveying. 3rd edition*, John Wiley and Sons.

Lutz, S., Schaer, S., Meindl, M., Dach, R. and Steigenberger, P. (2010). Higher-order Ionosphere Modeling for CODE's Next Reprocessing Activities. *Proceedings of the IGS Analysis Centre Workshop, Newcastle upon Tyne, England*.

Merrill, R. T. and McElhinny, M. W. (1983). *The Earth's Magnetic Field, its History, Origin and Planetary Perspective. International Geophysics series*, Volume 32. Academic Press Inc., 1983.

National Oceanic and Atmospheric Administration (NOAA) website. http://www.ngdc.noaa.gov/IAGA/vmod/igrf.html. Accessed June 2010.

Rowell, T. F. (2005). USTEC: A new product from the Space Environment Centre Characterizing the Ionospheric Total Electron Content. *GPS Solutions, Springer-Verlag*, **9**, 236–239.

Schaer, S., Beutler, G. and Rothacher, M. (1998). Mapping and Predicting The Ionosphere. *Proceedings of the IGS Analysis Centre Workshop, Darmstadt, Germany*.

Schaer, S. and Steigenberger, S. (2006). Determination and Use of GPS Differential Code Bias Values. *IGS Analysis Centre Workshop, Darmstadt, Germany*.